

# Wave-averaged geostrophic balance

Hossein A. Kafiabad<sup>1</sup>, Jacques Vanneste<sup>1</sup> and William R. Young<sup>2</sup>

<sup>1</sup>School of Mathematics and Maxwell Institute for Mathematical Sciences,  
University of Edinburgh, Edinburgh, UK

<sup>2</sup>Scripps Institution of Oceanography, University of California, San Diego, USA

## Abstract

In the presence of inertia-gravity waves, the geostrophic and hydrostatic balance that characterises the slow dynamics of rapidly rotating, strongly stratified flows holds in a time-averaged sense and applies to the Lagrangian-mean velocity and buoyancy. We give an elementary derivation of this wave-averaged balance and demonstrate its accuracy in numerical solutions of the three-dimensional Boussinesq equations, using a simple configuration in which vertically planar near-inertial waves interact with a barotropic anticyclonic vortex. We further use the conservation of the wave-averaged potential vorticity to predict the change in the barotropic vortex induced by the waves. Order-of-magnitude estimates based on these results suggest that Stokes drift associated with near-inertial waves is a non-negligible part of the sea-surface geostrophic velocity inferred from satellite altimetric measurements of sea-surface height.

## 1 Introduction

Our understanding of the large-scale dynamics of the atmosphere and ocean rests on the concept of geostrophic balance: motion with timescales much longer than the inertial timescale  $f^{-1}$ , with  $f$  the Coriolis parameter, is assumed to dominate, resulting in the familiar balance between Coriolis force and pressure gradients. The idea of dominant slow motion has stimulated decades of research extending balance beyond geostrophy to define dynamics which filter out fast motion to a high degree of accuracy – that is, dynamics restricted to a suitably defined slow manifold (e.g. Leith, 1980; Allen and Newberger, 1993; Warn et al., 1995; Vanneste, 2013; Kafiabad and Bartello, 2017). However, the amplitude of the fast motion, e.g. in the form of inertia-gravity waves, can often be large. For instance, the velocities associated with wind-driven inertial waves in the ocean frequently exceed those of the (vortical) balanced motion (e.g. Alford et al., 2016). There is, therefore, a need to reassess the notion of balance to account for the impact of waves. This can be achieved using reduced models which, rather than filtering the waves, average over their rapidly oscillating phases to describe the slow interactions between waves and vortical flow. We refer to these models as *wave-averaged* models.

Bretherton (1971), Grimshaw (1975) and, more recently, Wagner and Young (2015) showed that wave averaging naturally leads to a generalised-Lagrangian-mean (GLM) description of the flow, in which averaging is carried out at fixed particle label rather than fixed Eulerian position. Wave-averaged models can therefore be interpreted as approximations to the GLM equations of Andrews and McIntyre (1978) (see Bühler 2009 for an introduction to GLM). The wave-averaged models of interactions between near-inertial waves (NIWs) and quasigeostrophic flow derived by Xie and Vanneste (2015) and Wagner and Young (2016) fall into this category. Salmon (2016) provides an interesting variational perspective into this class of models in which weakly nonlinear internal waves interact perturbatively with quasigeostrophic flow.

One of the most striking predictions of wave-averaged and GLM theories is that a form of hydrostatic and geostrophic balance continues to hold in the presence of strong waves, but that this balance applies to the Lagrangian mean flow, in the sense that

$$f \mathbf{z} \times \bar{\mathbf{u}}^L = -\nabla \bar{\pi} + \bar{b}^L \mathbf{z}, \quad (1)$$

$f$	$N$	$a$	$m$	$Ro$	$Bu$	$E_0$	$\nu_h$	$\nu_z$
200	1600	0.45	8	0.04	0.0067	0.5	$5 \times 10^{-18}$	$5 \times 10^{-23}$

Table 1: Simulation parameters.

where  $\mathbf{z}$  is the vertical unit vector,  $\overline{\mathbf{u}}^L$  and  $\overline{b}^L$  are the Lagrangian-mean velocity and buoyancy, and  $\overline{\pi}$  is a mean pressure-like scalar (Moore, 1970; Andrews and McIntyre, 1978; Xie and Vanneste, 2015; Wagner and Young, 2015; Gilbert and Vanneste, 2018; Thomas et al., 2018). The Lagrangian-mean velocity is the sum of Eulerian-mean and Stokes velocities,

$$\overline{\mathbf{u}}^L = \overline{\mathbf{u}} + \overline{\mathbf{u}}^S, \quad \text{where } \overline{\mathbf{u}}^S = \overline{\boldsymbol{\xi}' \cdot \nabla \mathbf{u}'}, \quad (2)$$

with  $\boldsymbol{\xi}'$  and  $\mathbf{u}' = \boldsymbol{\xi}'_t$  denoting wave displacement and velocity and the overline denoting (Eulerian) time averaging. The appearance of the Stokes velocity  $\overline{\mathbf{u}}^S$  in the Coriolis term implies the existence of the Stokes–Coriolis force  $f\mathbf{z} \times \overline{\mathbf{u}}^S$  whose importance for shallow currents driven by surface gravity waves has long been recognised (e.g. Ursell and Deacon, 1950; Hasselmann, 1970; Huang, 1979; Leibovich, 1980). Here we are concerned with the Stokes–Coriolis force associated with internal gravity waves which also operates in the interior ocean. Equation (1) is a remarkable generalisation of the familiar geostrophic balance, with practical implications, e.g. for the interpretation of ocean velocities inferred from satellite altimetry data, yet (1) is not widely known. Another prediction of wave-averaged and GLM theories is the material conservation of a form of potential vorticity (PV) which combines the PV of the mean flow with a wave contribution. Together with (1) this leads to a wave-averaged form of quasigeostrophic dynamics which captures the feedback that waves exert on the mean flow.

The aim of this paper is to demonstrate the validity and usefulness of the wave-averaged geostrophic balance and PV conservation by testing these relations against numerical solutions of the three-dimensional Boussinesq equations. Applying wave-averaged relations to numerical simulations poses difficulties related to the definition of a suitable time average and the estimation of particle displacements  $\boldsymbol{\xi}'$  in (2). We sidestep these difficulties by focussing on a simple configuration: an inertial wave, initially with no horizontal dependence and the vertical structure of a plane travelling wave, is superimposed on an axisymmetric (Gaussian) barotropic anticyclonic vortex. This configuration has the advantage that, because the inertial wave is approximately linear, it retains a simple vertical and temporal structure proportional to  $e^{i(mz - ft)}$ , with  $m$  the vertical wavenumber. Time averaging can therefore be replaced by a straightforward vertical averaging and the mean component of the flow be identified with the barotropic component. Moreover, it turns out that for NIWs, the Stokes drift  $\overline{\mathbf{u}}^S$  can be deduced from the wave kinetic energy, thus circumventing the need to estimate the displacements  $\boldsymbol{\xi}'$ .

We describe our numerical simulation of the interaction between NIWs and an anticyclonic vortex in §2. The wave evolution follows a broadly understood scenario: after a rapid adjustment, wave energy concentrates in the vortex core, giving rise to an approximately axisymmetric trapped structure which is modulated periodically in time (Llewellyn Smith, 1999). Our focus is on the response of the mean flow to this wave pattern. In §3, we briefly sketch a derivation of the wave-averaged geostrophic balance (1) and of the form of the wave-averaged PV. Particularising this to the case of vertically planar inertial wave following Rocha et al. (2018) we relate (i) mean vertical vorticity, mean pressure and wave energy, and (ii) wave-induced change of mean vorticity to wave energy. We assess the accuracy of these two predictions in numerical solutions and find a remarkably good agreement in spite of the strong scaling assumptions required by the theory and the complexity of the full three-dimensional Boussinesq model. Our results demonstrate the value of wave-averaged theories for the analysis of geophysical flows in the context of three-dimensional nonlinear dynamics.

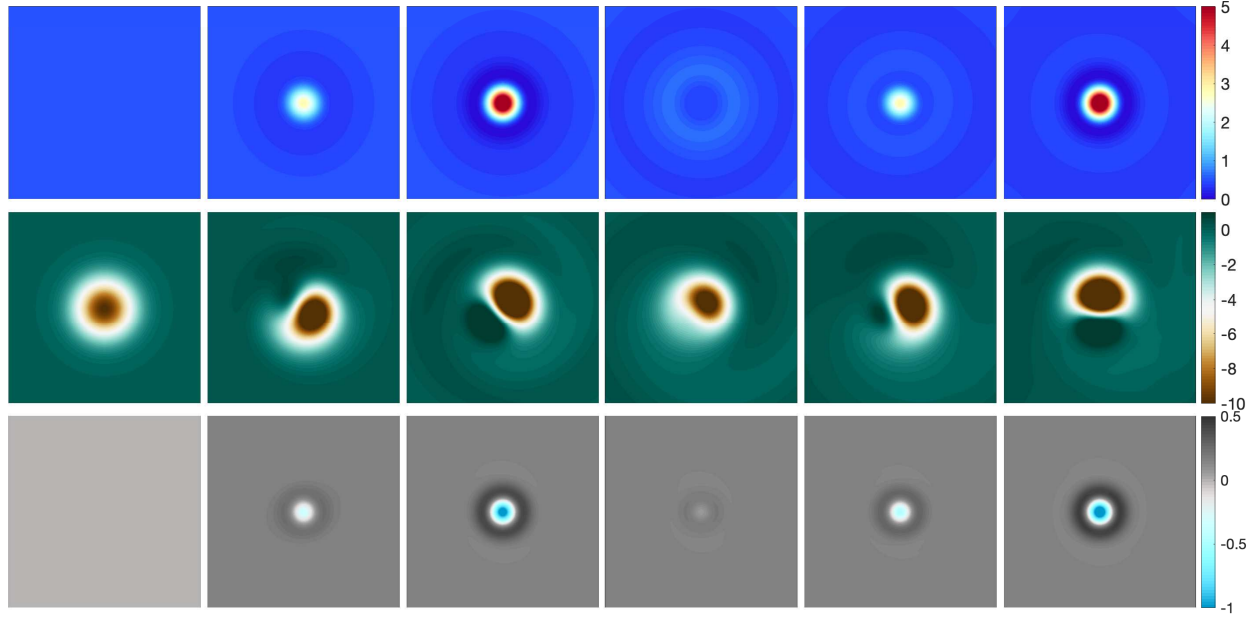


Figure 1: Horizontal slices of wave kinetic energy  $(u'^2 + v'^2)/2$  (top row), vertical vorticity  $\zeta$  (middle row) and change in Eulerian-mean vertical vorticity  $\bar{\zeta} - \zeta_0$  (bottom row) at times (from left to right)  $t = 0, 20.4, 43.2, 76.3, 99.2$  and  $122.1$  inertial periods  $2\pi/f$ .

## 2 Numerical solution of the Boussinesq equations

We analyse solutions of the non-hydrostatic Boussinesq equations for an initial condition consisting of a NIW superimposed on a barotropic anticyclonic vortex with the initial vertical vorticity

$$\zeta_0(r) = -Ro f e^{-r^2/a^2}, \quad (3)$$

where  $r$  is the radial coordinate,  $a$  the vortex radius, and  $Ro$  the maximum Rossby number,

$$Ro = |\zeta_0|_{\max}/f. \quad (4)$$

The NIW is initially horizontally uniform, with vertical structure  $e^{imz}$  with vertical wavenumber  $m$  and initial energy  $E_0$ . In addition to the Rossby number, the flow is characterised by the Burger number

$$Bu = N^2/(fma)^2, \quad (5)$$

where the inverse wavenumber  $m^{-1}$  and vortex radius  $a$  are used to define the characteristic vertical and horizontal scales. We focus on the regime where both  $Ro$  and  $Bu$  are small as required for nearly geostrophic mean dynamics and NIW dynamics.

The Boussinesq equations are solved in a triply periodic domain, using a code adapted from that of Waite and Bartello (2006), which relies on a de-aliased pseudospectral method and a third-order Adams–Bashforth scheme with time step  $0.06/f$ . The  $(2\pi)^2 \times 2\pi/36$  domain is discretised using a  $1152^2 \times 96$  uniform grid. A hyperdissipation of the form  $\nu_h(\partial_x^2 + \partial_y^2)^4 + \nu_z\partial_z^8$  is used for the momentum and density equations. The simulation parameters are listed in table 1. The domain size is much larger than the vortex radius ( $L/a \approx 14$ ) to mitigate the effect of waves re-entering from the boundaries.

The evolution of the NIW in the presence of a vortex is illustrated by the sequence of snapshots of horizontal slices shown in figure 1. The wave kinetic energy  $(u'^2 + v'^2)/2$  is displayed in the top row, the vertical vorticity in the middle row, and the (barotropic) mean vorticity in the bottom row (this is

also the Eulerian mean vorticity). Wave energy focusses in the vortex core, leading to an approximately axisymmetric trapped structure; this is a finite-amplitude, near-inertial normal mode of the vortex. The wave-energy concentration is modulated periodically in time, with a period much larger than the inertial period. The dynamics of the vertical vorticity  $\zeta$  is dominated by the fast oscillation at the inertial frequency induced by advection by the wave velocity. This oscillation is filtered out by vertical averaging, leaving an Eulerian mean vorticity  $\bar{\zeta}$  that is almost axisymmetric and oscillates slowly in unison with the wave energy. We next show how this mean dynamics can be explained using wave averaging.

### 3 Wave-averaged analysis

We first derive the wave-averaged geostrophic balance (1) and wave-averaged PV conservation for general inertia-gravity waves, then consider their application to NIWs and the numerical solution of §2.

#### 3.1 Wave-averaged geostrophy and potential-vorticity conservation

We provide only an informal sketch of the derivation and refer the reader to Wagner and Young (2015) for details (see Thomas et al. (2018) for related shallow-water results). We start with the Boussinesq equations

$$D_t \mathbf{u} + f \mathbf{z} \times \mathbf{u} = -\nabla p + b \mathbf{z}, \quad (6a)$$

$$D_t b + N^2 w = 0, \quad (6b)$$

$$\nabla \cdot \mathbf{u} = 0, \quad (6c)$$

where  $D_t = \partial_t + \mathbf{u} \cdot \nabla$ . For simplicity we take the Brunt–Väisälä frequency  $N$  constant (see Wagner and Young (2015) for the non-constant case).

We assume that the flow consists of fast waves, with small amplitude  $\varepsilon \ll 1$ , interacting with a slow flow, with smaller amplitude  $\varepsilon^2$ . This is the *strong-wave* assumption which makes it possible to capture the impact of the waves on the flow without the need to carry out the perturbation expansion to an unwieldy high order. We expand the velocity as

$$\mathbf{u} = \varepsilon \mathbf{u}' + \varepsilon^2 \bar{\mathbf{u}} + \dots \quad (7)$$

and the other dynamical fields likewise. Here the prime identifies the wave component, the overbar the mean component obtained by averaging over the fast wave timescale, and the dots include a rapidly varying  $O(\varepsilon^2)$  term as well as  $O(\varepsilon^3)$  terms. Introducing (7) into (6) gives, at  $O(\varepsilon)$ , the linear inertia-gravity-wave equations

$$u'_t - f v' = -p'_x, \quad v'_t + f u' = -p'_y, \quad w'_t - b = -p'_z, \quad (8a)$$

$$b'_t + N^2 w' = 0, \quad \nabla \cdot \mathbf{u}' = 0. \quad (8b)$$

Averaging the next-order equation gives

$$\overline{\mathbf{u}' \cdot \nabla \mathbf{u}'} - f \bar{v} = -\bar{p}_x, \quad \overline{\mathbf{u}' \cdot \nabla v'} + f \bar{u} = -\bar{p}_y, \quad \overline{\mathbf{u}' \cdot \nabla w'} - \bar{b} = -\bar{p}_z, \quad (9a)$$

$$\overline{\mathbf{u}' \cdot \nabla b'} + N^2 \bar{w} = 0, \quad \nabla \cdot \bar{\mathbf{u}} = 0. \quad (9b)$$

Defining the wave displacement  $\boldsymbol{\xi}'$  with  $\boldsymbol{\xi}'_t = \mathbf{u}'$ , we can rewrite the nonlinear terms in (9a) in terms of  $\boldsymbol{\xi}'$ . For instance, we have

$$\overline{\mathbf{u}' \cdot \nabla \mathbf{u}'} = -\overline{\boldsymbol{\xi}' \cdot \nabla u'_t} = -f \overline{\boldsymbol{\xi}' \cdot \nabla v'} + \overline{\boldsymbol{\xi}' \cdot \nabla p'_x}. \quad (10)$$

The remarkable identity established in Wagner and Young (2015) and Appendix A,

$$\overline{(\boldsymbol{\xi}' \cdot \nabla) \nabla p'} = \frac{1}{2} \nabla (\overline{\boldsymbol{\xi}' \cdot \nabla p'}) = \frac{1}{2} \nabla \bar{p}^S \quad (11)$$

with  $\bar{p}^S = \overline{\boldsymbol{\xi}' \cdot \nabla p'}$  the Stokes pressure, then reduces (9a) to (1) with

$$\bar{b}^L = \bar{b} + \bar{b}^S \quad \text{and} \quad \bar{\pi} = \bar{p} + \frac{1}{2} \bar{p}^S, \quad (12)$$

where  $\bar{b}^S = \overline{\boldsymbol{\xi}' \cdot \nabla b'}$  is the Stokes buoyancy. The mean buoyancy equation in (9b) can also be simplified to obtain

$$\bar{w}^L = \bar{w} + \overline{\boldsymbol{\xi}' \cdot \nabla w'} = \bar{w} + \bar{w}^S, \quad (13a)$$

$$= 0. \quad (13b)$$

It is natural to introduce the streamfunction  $L\psi = \bar{\pi}/f$  to write the wave-averaged balance relations (1) in the form

$$\bar{\mathbf{u}}^L = (-L\psi_y, L\psi_x, 0) \quad \text{and} \quad \bar{b}^L = L\psi_z, \quad (14)$$

mirroring the familiar geostrophic and hydrostatic relations. The vorticity of the Lagrangian-mean flow is then

$$L\zeta = \bar{v}_x^L - \bar{u}_y^L = \Delta L\psi, \quad (15)$$

where  $\Delta = \partial_x^2 + \partial_y^2$  is the horizontal Laplacian. We emphasise that  $L\psi$  and  $L\zeta$  are the streamfunction and vorticity corresponding the Lagrangian-mean velocity  $(\bar{u}^L, \bar{v}^L)$  but are not themselves Lagrangian means of any specific fields. This is evident from the factor 1/2 in (12) and the fact that  $L\zeta \neq \bar{\zeta} + \overline{\boldsymbol{\xi}' \cdot \nabla \zeta'}$  (the difference is related to the curl of the pseudomomentum, see e.g. Bühler (2009) or Gilbert and Vanneste (2018)).

We can go beyond the diagnostic relation (14) and make dynamical predictions using the conservation of PV. After removing the constant contribution  $N^2 f$  and scaling by  $N^2$ , the PV can be written as

$$q = v_x - u_y + fb_z/N^2 + (\nabla \times \mathbf{u}) \cdot \nabla b/N^2. \quad (16)$$

This is an  $O(\varepsilon^2)$ , slow quantity, approximately equal to its time average with which we identify it to write the leading-order wave-averaged PV as

$$q = L\zeta + f^2 L\psi_{zz}/N^2 \underbrace{- \bar{v}_x^S + \bar{u}_y^S - f \bar{b}_z^S/N^2 + \overline{(\nabla \times \mathbf{u}') \cdot \nabla b'/N^2}}_{q^w}, \quad (17)$$

where (14) has been used. The first two terms on the right of (17) make up the familiar quasi-geostrophic PV, here involving the streamfunction of the Lagrangian-mean flow. The remaining terms constitute the wave PV denoted  $q^w$ . We note that the wave-averaged geostrophic balance and PV conservation also follow directly from GLM theory (Andrews and McIntyre, 1978; Bühler and McIntyre, 1998; Holmes-Cerfon et al., 2011; Xie and Vanneste, 2015; Gilbert and Vanneste, 2018).

### 3.2 Application to near-inertial-wave-vortex interaction

The horizontal velocity  $(u', v')$  of the vertically planar NIWs excited in our simulation can be written in the complex form

$$u'(x, y, z, t) + i v'(x, y, z, t) = \phi(x, y, t) e^{i(mz - ft)}, \quad (18)$$

where  $\phi$  is a slowly-varying complex amplitude, also known as the back-rotated velocity. This form is exact for linear waves and an excellent approximation for the waves in our simulation. It makes clear that vertical averaging is equivalent to time averaging over the fast wave timescale. The wave kinetic energy is  $(u'^2 + v'^2)/2 = |\phi|^2/2$  and thus the top row of figure 1 shows the evolution of  $|\phi|^2/2$ .

Equation (1) for wave-averaged geostrophy simplifies dramatically for NIWs of the form (18). First,  $p' \approx 0$  for NIWs, so  $\bar{\pi} = \bar{p}$ . Taking the horizontal divergence of (1) then gives

$$f L\zeta = \Delta \bar{p}. \quad (19)$$

Second, for vertically plane NIWs the horizontal part of the Stokes velocity can be computed as

$$(\bar{u}^S, \bar{v}^S) = (\mathcal{A}_y, -\mathcal{A}_x), \quad \text{where} \quad \mathcal{A} = |\phi|^2/(2f) \quad (20)$$

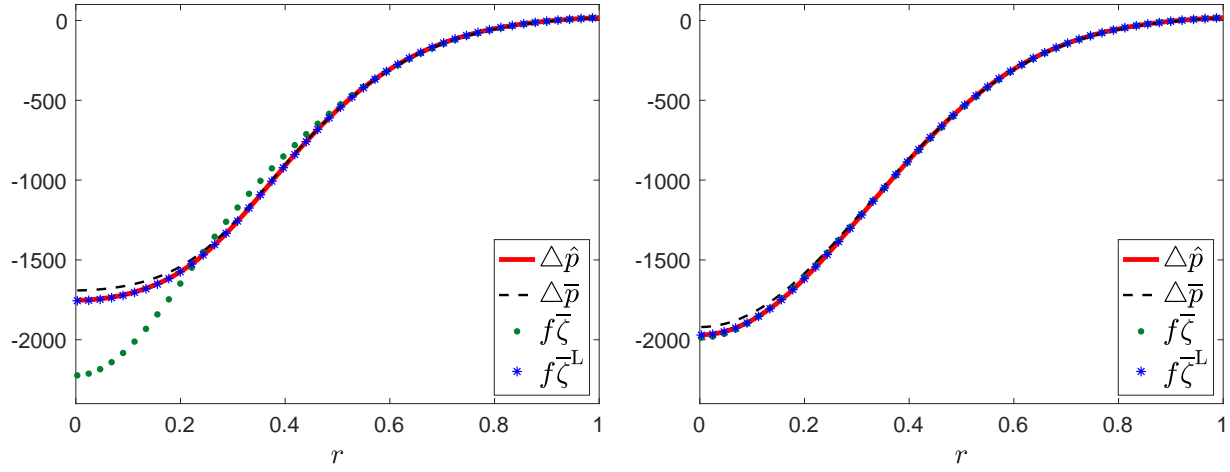


Figure 2: Radial profiles of the Laplacian of the mean pressure  $\bar{p}$  and mean modified pressure  $\hat{p}$ , and of  $f$  times the Lagrangian- and Eulerian-mean vertical vorticity for  $t = 43.2$  (left) and  $76.3$  (right) inertial periods.

is the wave action density, whose negative plays the role of a streamfunction for the Stokes velocity (see Rocha et al., 2018, and Appendix A). Combining (19) and (20) relates the Eulerian-mean vertical vorticity to the pressure according to

$$f(\bar{\zeta} - \Delta\mathcal{A}) = \Delta\bar{p}. \quad (21)$$

This is the form of wave-averaged geostrophy that we test in our numerical simulation. Figure 2 shows radial profiles (obtained by azimuthal averaging) of the Eulerian-mean vorticity  $\bar{\zeta}$ , vorticity of the Lagrangian-mean flow, computed as  $\bar{\zeta}^L = \bar{\zeta} - \Delta\mathcal{A}$ , and horizontal Laplacian of mean pressure  $\Delta\bar{p}$ . These are shown at two different times corresponding to a maximum in the wave-energy concentration (left) and to a nearly uniform wave field (right). The mean pressure is computed by solving the Poisson equation obtained by taking the divergence of the mean horizontal momentum equation; a modified pressure  $\hat{p}$ , computed using only the baroclinic (wave) component of the velocity, is also shown. It is clear from the figure that, when the wave energy is non-uniform, geostrophic balance holds to a much better accuracy in the wave-averaged sense (19) than in the conventional sense, that is, for the Lagrangian-mean velocity rather than for the Eulerian-mean velocity. The match is better still when the modified pressure is used; this is because its definition removes a contribution to the pressure associated with an ageostrophic balanced component of the mean flow (primarily the cyclostrophic correction to geostrophy) which our small-Rossby theory does not account for.

For NIWs, the wave part of the PV (17) can be expressed in terms of  $\phi$ , retaining only leading-order terms in the small Burger number to obtain

$$q = \mathbf{L}\zeta + f^2 \mathbf{L}\psi_{zz}/N^2 + \Delta|\phi|^2/(4f) + \mathbf{i}\partial(\phi, \phi^*)/(2f), \quad (22)$$

where  $\partial(\cdot, \cdot)$  denotes the Jacobian operator (see Xie and Vanneste, 2015; Wagner and Young, 2016). For an axisymmetric wave field  $\phi(r, t)$  and barotropic mean flow this reduces to

$$q = \mathbf{L}\zeta + \Delta\mathcal{A}/2, \quad (23)$$

where  $\Delta(\cdot) = r^{-1}\partial_r(r\partial_r\cdot)$ . For waves that are initially uniform in the horizontal, the Stokes drift and horizontal Laplacian vanish initially, so the conservation of  $q$  – which holds pointwise on our axisymmetric setup – implies

$$\mathbf{L}\zeta + \Delta\mathcal{A}/2 = \zeta_0, \quad (24)$$

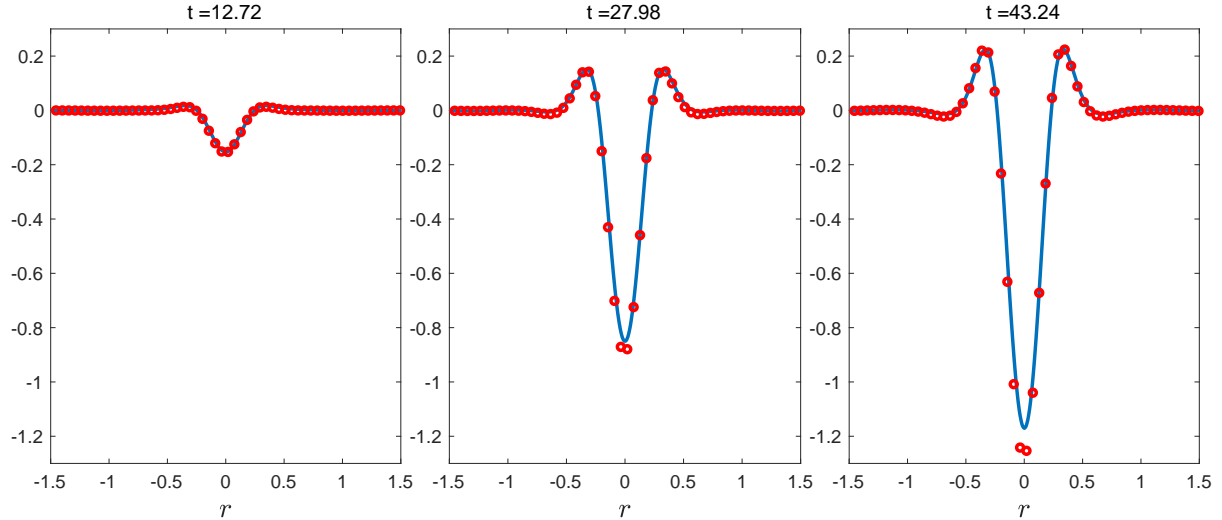


Figure 3: Comparison of mean-vorticity change  $\bar{\zeta} - \zeta_0$  ( $\circ$ ) with  $\Delta\mathcal{A}/2$  (solid line) along a radial line and for  $t = 12.7$  (left), 30 (middle) and 43.2 (right) inertial periods.

where  $\zeta_0(r)$  is the initial vertical vorticity. Using (20) this gives the prediction

$$\bar{\zeta} = \zeta_0 + \Delta\mathcal{A}/2. \quad (25)$$

This result explains the correlation between the evolution of the wave kinetic energy  $(u'^2 + v'^2)/2 = f\mathcal{A}$  and  $\bar{\zeta}$  observed in figure 1. We test (25) quantitatively in figure 3 by comparing the change in mean vorticity,  $\bar{\zeta} - \zeta_0$ , with  $\Delta\mathcal{A}/2$  at three different times corresponding to different phases in the oscillation of wave energy. The good match between the two quantities confirms the validity of (25). Thus conservation of wave-averaged PV predicts the dynamics of the mean flow in the presence of waves with substantial amplitude.

## 4 Conclusion

This paper examines the way geostrophic balance – a cornerstone of geophysical fluid dynamics – is altered in the presence of inertia-gravity waves to become a balance between the Coriolis force associated with the Lagrangian-mean velocity and a modified mean pressure. The wave-induced correction to geostrophy has long been known (e.g. Moore, 1970) but it has received much less attention than the issue of finite-Rossby-number corrections associated with higher-order balance (e.g. Machenhauer, 1977; Allen and Newberger, 1993; McIntyre and Norton, 2000; Mohebalhojeh and Dritschel, 2001; Kafiabad and Bartello, 2018). By focusing on numerical simulations in a very simple setup, in which vertically NIW waves are superimposed on a barotropic vortex, we are able to demonstrate unambiguously that the wave-induced correction matters and, for NIWs, can be estimated from the wave energy, consistent with theoretical predictions. We further show that the material conservation of a wave-averaged PV can be exploited to predict mean-flow changes from the wave energy.

It is of interest to estimate the size of the wave-induced correction, that is, the size of the NIW Stokes drift, in a realistic context. Let us consider the case of NIWs in the ocean’s mixed layer represented, as is standard, by a slab model (e.g. Alford et al., 2016). We note that the relation  $\bar{\mathbf{u}}^L = (-\mathcal{A}_y, \mathcal{A}_x)$  applies to (vertically independent) waves in a slab model as well as to the vertically planar waves considered above. We estimate  $\mathcal{A}$  from the values of inertial-wave kinetic energy inferred by Chaigneau et al. (2008) from drifter data. In parts of the ocean with strong wind forcing, they found this kinetic energy to be of the order of  $10^3 \text{ J m}^{-2}$ . This corresponds to  $(u'^2 + v'^2)/2 = 10^3/(\rho h) \approx 10^{-2} \text{ m}^2 \text{ s}^{-2}$ , taking the water density  $\rho = 10^3 \text{ kg m}^{-3}$  and mixed-layer depth  $h = 100 \text{ m}$ , and hence  $\mathcal{A} \approx 10^2 \text{ m}^2 \text{ s}^{-1}$  for  $f = 10^{-4} \text{ s}^{-1}$ . Using a spatial scale of 10

km based on recent simulations of NIWs (Asselin and Young, 2019), we finally estimate  $|\overline{\mathbf{u}}^S| \approx 10^{-2} \text{ m s}^{-1}$ , a substantial fraction of typical geostrophic velocities at the ocean surface. Larger values are obtained for smaller  $f$  (lower latitudes) and a shallower mixed layer. This suggests that Stokes drift associated with NIWs is a non-negligible part of the sea-surface geostrophic velocity inferred from satellite altimetric measurements of sea-surface height. The NIW Stokes velocity is also comparable in magnitude to the Stokes drift of the surface gravity waves; unlike the latter, it extends across the mixed layer and in the ocean interior, hence it is potentially more important for transport.

We conclude by noting that, while the present paper concentrates on the relation between wave energy and wave-induced mean-flow, it is also desirable to analyse the mechanism that leads to the wave-energy oscillations seen in figure 1. We leave this analysis for future work.

**Acknowledgments.** HAK and JV are supported by the UK Natural Environment Research Council grant NE/R006652/1. WRY is supported by the National Science Foundation Award OCE-1657041. This work used the ARCHER UK National Supercomputing Service.

**Declaration of interests.** The authors report no conflict of interest.

## A Derivation details

We establish (11) by rewriting the wave momentum equation (8a) as

$$\nabla p' = \mathbf{L} \boldsymbol{\xi}', \quad \text{where } \mathbf{L} = \begin{pmatrix} -\partial_t^2 & f\partial_t & 0 \\ -f\partial_t & -\partial_t^2 & 0 \\ 0 & 0 & -\partial_t^2 - N^2 \end{pmatrix}. \quad (26)$$

The linear operator  $\mathbf{L}$  is self-adjoint in the sense that  $\overline{\mathbf{a} \cdot \mathbf{L} \mathbf{b}} = \overline{\mathbf{b} \cdot \mathbf{L} \mathbf{a}}$  for arbitrary time-periodic vectors  $\mathbf{a}$  and  $\mathbf{b}$ . Using this we compute

$$\partial_i(\overline{\boldsymbol{\xi}' \cdot \nabla p'}) = \partial_i(\overline{\boldsymbol{\xi}' \cdot \mathbf{L} \boldsymbol{\xi}'} ) = 2\overline{\boldsymbol{\xi}' \cdot \mathbf{L} \partial_i \boldsymbol{\xi}'} = 2\overline{\boldsymbol{\xi}' \cdot \partial_i \nabla p'} = 2\overline{(\boldsymbol{\xi}' \cdot \nabla) \partial_i p'} \quad (27)$$

and (11) follows.

We now turn to (20). The unaveraged Stokes velocity is

$$(\boldsymbol{\xi}' \cdot \nabla) \mathbf{u}' = \partial_t \left[ \frac{1}{2} (\boldsymbol{\xi}' \cdot \nabla) \boldsymbol{\xi}' \right] - \frac{1}{2} \nabla \times \mathbf{h}, \quad (28)$$

where  $\mathbf{h} = \boldsymbol{\xi}' \times \mathbf{u}'$  is the angular momentum density, and we used the standard vector identity for the curl of a cross product and that  $\nabla \cdot \boldsymbol{\xi}' = \nabla \cdot \mathbf{u}' = 0$ . The time average of (28) gives the explicit solenoidal representation of the Stokes velocity

$$\overline{\mathbf{u}}^S = -\frac{1}{2} \nabla \times \overline{\mathbf{h}}. \quad (29)$$

For vertically planar waves,  $\partial_z \overline{\mathbf{h}} = 0$  hence

$$(\overline{u}^S, \overline{v}^S) = \frac{1}{2} (-\overline{h}_y, \overline{h}_x) \quad (30)$$

where  $\overline{h} = \overline{\xi' v' - \eta' u'}$  is the vertical component of  $\overline{\mathbf{h}}$ . For inertial waves,  $u'_t - f v' = v'_t + f u' = 0$ , so  $\overline{h} = (\xi' u'_t + \eta' v'_t)/f = -(\overline{u'^2} + \overline{v'^2})/f = -\mathcal{A}$  and (30) gives (20).

## References

- M. H. Alford, J. A. MacKinnon, H. L. Simmons, and J. D. Nash. Near-inertial internal gravity waves in the ocean. *Annual review of marine science*, 8:95–123, 2016.
- J. S. Allen and P. A. Newberger. On intermediate models for stratified flow. *Journal of Physical Oceanography*, 23(11):2462–2486, 1993.



- D. G. Andrews and M. E. McIntyre. An exact theory of nonlinear waves on a Lagrangian-mean flow. *Journal of Fluid Mechanics*, 89:609–646, 1978.
- O. Asselin and W. R. Young. Penetration of wind-generated near-inertial waves into a turbulent ocean. *arXiv preprint arXiv:1912.08323*, 2019.
- F. P. Bretherton. The general linearized theory of wave propagation. In *Mathematical Problems in the Geophysical Sciences*, volume 13 of *Lect. Appl. Math.*, pages 61–102. Am. Math. Soc., 1971.
- O. Bühler. *Waves and mean flows*. Cambridge University Press, 2009.
- O. Bühler and M. E. McIntyre. On non-dissipative wave–mean interactions in the atmosphere or oceans. *J. Fluid Mech.*, 354:301–343, 1998.
- A. Chaigneau, O. Pizarro, and W. Rojas. Global climatology of near-inertial current characteristics from Lagrangian observations. *Geophysical Research Letters*, 35(13), 2008.
- A. D. Gilbert and J. Vanneste. Geometric generalised Lagrangian-mean theories. *Journal of Fluid Mechanics*, 839:95–134, 2018.
- R. Grimshaw. Nonlinear internal gravity waves in a rotating fluid. *Journal of Fluid Mechanics*, 71(3): 497–512, 1975.
- K. Hasselmann. Wave-driven inertial oscillations. *Geophysical and Astrophysical Fluid Dynamics*, 1(3-4): 463–502, 1970.
- M. Holmes-Cerfon, O. Bühler, and R. Ferrari. Particle dispersion by random waves in the rotating boussinesq system. *J. Fluid Mech.*, 670:150–175, 2011.
- N. E. Huang. On surface drift currents in the ocean. *Journal of Fluid Mechanics*, 91(1):191–208, 1979.
- H. A. Kafiabad and P. Bartello. Rotating stratified turbulence and the slow manifold. *Computers & Fluids*, 151:23–34, 2017.
- H. A. Kafiabad and P. Bartello. Spontaneous imbalance in the non-hydrostatic boussinesq equations. *Journal of Fluid Mechanics*, 847:614–643, 2018.
- S. Leibovich. On wave-current interaction theories of langmuir circulations. *Journal of Fluid Mechanics*, 99 (4):715–724, 1980.
- C. Leith. Nonlinear normal mode initialization and quasi-geostrophic theory. *Journal of the Atmospheric Sciences*, 37(5):958–968, 1980.
- S. G. Llewellyn Smith. Near-inertial oscillations of a barotropic vortex: trapped modes and time evolution. *Journal of physical oceanography*, 29(4):747–761, 1999.
- B. Machenhauer. On the dynamics of gravity oscillations in a shallow water model with applications to normal mode initialization. *Beitr. Phys. Atmos*, 50:253–271, 1977.
- M. E. McIntyre and W. A. Norton. Potential vorticity inversion on a hemisphere. *J. Atmos. Sci.*, 57: 1214–1235, 2000. Corrigendum: **58**, 949-949 (2001).
- A. R. Mohebalhojeh and D. G. Dritschel. Hierarchies of balance conditions for the  $f$ -plane shallow water equations. *J. Atmos. Sci.*, 58:2411–2426, 2001.
- D. Moore. The mass transport velocity induced by free oscillations at a single frequency. *Geophysical Fluid Dynamics*, 1:237–247, 1970.

- C. B. Rocha, G. L. Wagner, and W. R. Young. Stimulated generation: extraction of energy from balanced flow by near-inertial waves. *Journal of Fluid Mechanics*, 847:417–451, 2018.
- R. Salmon. Variational treatment of inertia–gravity waves interacting with a quasi-geostrophic mean flow. *Journal of Fluid Mechanics*, 809:502–529, 2016.
- J. Thomas, O. Bühler, and K. S. Smith. Wave-induced mean flows in rotating shallow water with uniform potential vorticity. *Journal of Fluid Mechanics*, 839:408–429, 2018.
- F. Ursell and G. Deacon. On the theoretical form of ocean swell on a rotating earth. *Geophysical Journal International*, 6:1–8, 1950.
- J. Vanneste. Balance and spontaneous wave generation in geophysical flows. *Annu. Rev. Fluid Mech.*, 45:147–172, 2013.
- G. Wagner and W. Young. Available potential vorticity and wave-averaged quasi-geostrophic flow. *Journal of Fluid Mechanics*, 785:401–424, 2015.
- G. Wagner and W. Young. A three-component model for the coupled evolution of near-inertial waves, quasi-geostrophic flow and the near-inertial second harmonic. *Journal of Fluid Mechanics*, 802:806–837, 2016.
- M. L. Waite and P. Bartello. The transition from geostrophic to stratified turbulence. *Journal of Fluid Mechanics*, 568:89–108, 2006.
- T. Warn, O. Bokhove, T. G. Shepherd, and G. K. Vallis. Rossby number expansions, slaving principles, and balance dynamics. *Q. J. R. Meteor. Soc.*, 121:723–739, 1995.
- J.-H. Xie and J. Vanneste. A generalised-Lagrangian-mean model of the interactions between near-inertial waves and mean flow. *Journal of Fluid Mechanics*, 774:143–169, 2015.